BULLETIN OF THE POLISH ACADEMY OF SCIENCES
TECHNICAL SCIENCES, Vol. 72(2), 2024, Article number: e148840
DOI: 10.24425/bpasts.2024.148840

The clamping selection method to reduce the vibration of large-size workpieces during the face milling process

Krzysztof J. KALIŃSKI[1], Marek A. GALEWSKI[1], Natalia STAWICKA-MORAWSKA[1]*, Krzysztof JEMIELNIAK[2], and Michał R. MAZUR[1]

[1] Gdansk University of Technology, Faculty of Mechanical Engineering and Ship Technology, Institute of Mechanics and Machine Design, Gdansk, 80-233, Poland

[2] Warsaw University of Technology, Faculty of Mechanical and Industrial Engineering, Institute of Manufacturing Processes, Warsaw, 00-661, Poland

Abstract. The article introduces a method for selecting the best clamping conditions to obtain vibration reduction during the milling of large-size workpieces. It is based on experimental modal analysis performed for a set of assumed, fixing conditions of a considered workpiece to identify frequency response functions (FRFs) for each tightening torque of the mounting screws. Simulated plots of periodically changing nominal cutting forces are then calculated. Subsequently, by multiplying FRF and spectra of cutting forces, a clamping selection function (CSF) is determined, and, thanks to this function, vibration root mean square (RMS) is calculated resulting in the clamping selection indicator (CSI) that indicates the best clamping of the workpiece. The effectiveness of the method was evidenced by assessing the RMS value of the vibration level observed in the time domain during the real-time face milling process of a large-sized exemplary item. The proposed approach may be useful for seeking the best conditions for fixing the workpiece on the table.

Keywords: clamping selection indicator; milling vibrations; stiffness adjustment; experimental modal analysis.

1. INTRODUCTION

The vital issue during the machining is the demand for a product that fulfils, for example, desired geometrical and surface quality criteria. Unfortunately, this task, especially in the manufacturing of large-sized structures is challenging due to the occurrence of the relative vibrations of the tool-workpiece system [1]. For example, the surface texture quality, especially roughness, is strongly affected by the regeneration phenomenon, often observed during face milling [2].

There are various developed methods for vibration reduction during milling. Some of them concentrate on the problem of ensuring appropriate workpiece fixtures or the whole milling machine stiffness. For example, a chatter control strategy introducing asymmetric stiffness control in two directions of the spindle system was proposed in [3].

Another solution for ensuring the accurate stiffness of the machine tool foundation for machining large-size components relies on the optimized tightening sequence of the anchor bolts according to a given configuration of the anchor system and machine bed [4]. Nevertheless, to enhance the surface quality during the face milling process, more essential aspects involve optimizing the mounting pattern of the workpiece on the machine table considering the structure of variable stiffness [5]. Moreover, it must be noted that workpiece holders may also influence surface quality, tool wear, and energy consumption during milling operations [6–8].

Other solutions are elastomeric layers that clamp the workpiece and dampen the machining process [9] and vacuum tables that may clamp various types of workpieces and reduce vibrations [10]. The vacuum holding fixtures are one of the most common industrial solutions [11], especially for large-size, thin-walled workpieces. In [12] a moving fixture and in [13] a moving magnetic clamping device were designed to support the flexible workpieces. Very good result in suppressing chatter was also achieved with composite, mechanical, and magnetorheological clamping [14].

Another method for controlling deformations of thin-walled parts was proposed in [15]. The stiffness of the workpiece during machining was obtained by the stiffness updating method using an algorithm for optimizing the cutter orientation in order to match the force to the direction of maximum stiffness. The best cutter orientation is obtained by adopting the artificial intelligence-based, quantum Particle Swarm Optimization algorithm.

Due to the complex character of vibrations during large-size workpiece milling, the recommended solution cannot be limited only to chatter vibration. Therefore, a dedicated approach

*e-mail: natalia.morawska@pg.edu.pl

Manuscript submitted 2022-11-01, revised 2023-11-01, initially accepted for publication 2023-12-08, published in March 2024.

should consider not only the natural frequencies accompanying the identified system poles but also the more important and more noticeable impact of harmonic frequencies of excited vibrations [16].

A study investigating the impact of the milling parameters and the tool position on surface roughness and process vibration in a configuration with limited rigidity was conducted [17]. However, a complete force model is needed because the cutting force plays a key role, significantly affecting tool wear, workpiece deformation, and surface finish [18].

This paper focuses on the methodology based on looking for conditions that minimize the vibration at a tool-flexible workpiece conventional contact point. This is achieved with the same geometric and kinematic milling parameters but with different stiffness of the workpiece mounting. This is a significant modification of the idea presented in [19,20], which involves considering the periodically changing position of cutting forces coming from the tool teeth temporarily cooperating with the workpiece. At this point, it is also worth mentioning the possibility of suppressing the machining vibration of the flexible workpiece by designing an appropriate fixture layout scheme [21,22]. Unlike these methods, changing the conditions of mounting the object described in this paper involves tightening the mounting screws with an appropriate torque of a repeatable value. The above does not require the construction of an additional holder for mounting a large-sized object, which would be a much more difficult and much more expensive task, especially during research performed in industrial conditions. In the presented approach, only variants of the standard fixture are considered in order to choose the best one out of them, i.e. the one that results in the lowest vibrations during milling.

2. METHODOLOGY

The proposed method is intended to determine the best clamping conditions for the machined workpiece using experimental modal analysis of the workpiece, conducted to identify its frequency response functions (FRFs), as well as simulated plots of periodically changing nominal cutting forces. The suggested method consists in empirically determining, due to the repeatability of the mounting, the influence of the tightening torque of the mounting screws on the experimentally determined FRF. Since the method does not require knowledge of the milling computational model, its implementation meets the requirement of incurring minimal financial costs.

The proposed procedure includes (Fig. 1):

- Determination of simulated functions of amplitude spectra of periodically changing cutting forces, perpendicular to the milled surface.
- Measurement of FRF of a workpiece mounted on a machine tool table, on the surface intended for milling.
- Multiplication of the amplitude spectrum of the function of cutting forces and FRF of the workpiece to obtain clamping selection function (CSF).
- Determination of the clamping selection indicator (CSI) as the RMS of the time course of the workpiece displacement function (directly from the spectrum, without inverse FFT).
- Determination of the best solution to mounting the workpiece, based on the CSI minimum value, for a direction perpendicular to the milled surface. This is a completely new, authorial approach that has not been made available anywhere before. It represents significant progress over the previous developments [19,20], thanks to the consideration of a periodically changing position of the tool teeth currently cooperating with the workpiece.
- Performance of the target milling process due to the best solution of mounting the workpiece.

The advisability of calculating the displacement function along the width of the undeformed chip is dictated with dignity with vibrations perpendicular to the machined surface, directly affecting its quality (shape deviations, roughness). The smaller the vibration along the width of the undeformed chip, the better the milling process is.

The equations defining the behavior of tool and workpiece interaction during the milling process are universal (Fig. 2) because they consider cutting forces acting in different directions.

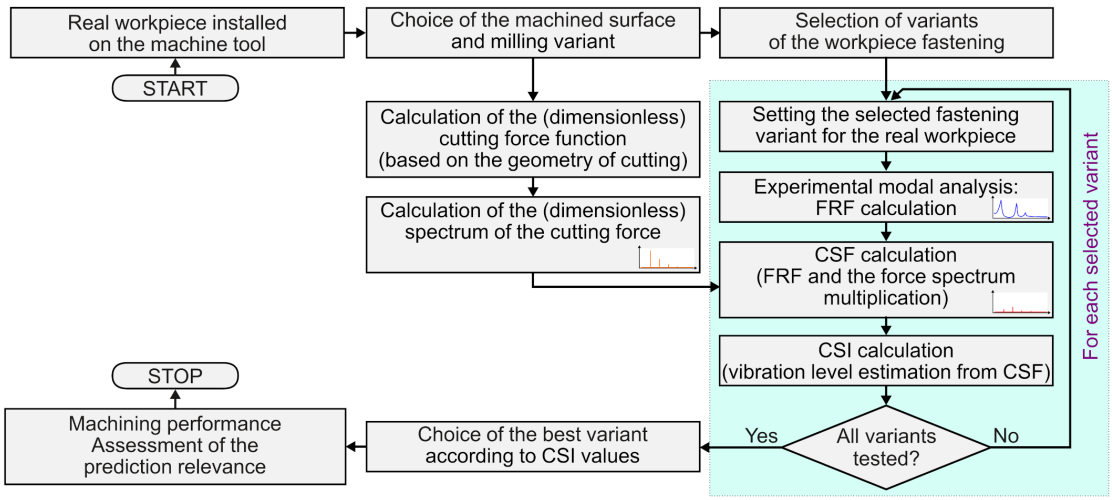

Fig. 1. Block diagram of the procedure for searching the best conditions for clamping the workpiece by estimating the minimum value of CSI

The computational model also includes non-linear and non-stationary effects. These effects make the problem of searching for the best clamping conditions that minimize vibration levels much more difficult. To simplify the problem, additional assumptions are proposed to be made, i.e.:

- Consideration of the uniform pitch cutting tool with periodically changing teeth positions relative to the workpiece. Naturally, this states a certain simplification of the milling process dynamics, but it aims to provide a description disregarding the alteration of the structure arrangement over time.
- Assuming the hypothesis that the vibration level of the workpiece in the direction normal to the machined surface is determined by the cutting forces of the edges i_l temporary establishing contact with the workpiece, while the cutting force of the edge no. l, $l = 1,\ldots,i_l$ (modelled as a coupling element, CE no. l [20]) acts in the direction of the width of the undeformed chip y_{l3}, while the phenomena in the other directions, i.e. thickness of the undeformed chip y_{l2} and the cutting speed y_{l1}, are neglected. The above also justifies the noticeable nose radius (e.g. 0.8 mm) of the edge, important especially at a small depth of cut a_p (e.g. 1 mm).
- The dynamic changes in undeformed chip thickness ($\Delta h_l(t)$) are omitted, i.e. $h_l(t) = h_{Dl}(t)$. Results of the vibration measurements conducted for various tested cases of milling flat surfaces indicated that all of them involved a stable machining process, with no signs of chatter vibration. These observations support the concept of neglecting regenerative vibration along the undeformed chip thickness, especially the regenerative influence of the tool path, which could potentially lead to stability issues and the development of chatter vibration.
- Vibration along the undeformed chip width is much smaller than its nominal value ($|\Delta b_l(t)| \ll b_D$) which is the case encountered when milling large-sized workpieces.

Adopting the above assumptions means simplifying the description of the interaction between the cutting tool edge no. *l* and the workpiece only to the concentrated force acting in the direction of the width of the undeformed chip, the value of which results from the given cutting conditions of the milling process, i.e. [20]:

$$F_{yl3}(t) = \begin{cases} \mu_{l3} k_{dl} b_D h_{Dl}(t), & h_{Dl}(t) > 0, \\ 0, & h_{Dl}(t) \le 0, \end{cases} \tag{1}$$

and

$$h_{Dl}(t) = \begin{cases} f_z \sin\kappa_r \cos\varphi_l(t), & \varphi_{ll} \le \varphi_l(t) \le \varphi_{ul}, \\ 0, & \varphi_{ll} > \varphi_l(t) \vee \varphi_l(t) > \varphi_{ul}, \end{cases} \tag{2}$$

$$\varphi_l(t) = \begin{cases} \dfrac{2\pi n}{60} t + \varphi_1 + (l-1)\dfrac{2\pi}{z} \\ \quad \text{for } \dfrac{2\pi n}{60} t + \varphi_1 + (l-1)\dfrac{2\pi}{z} \text{ modulo } 2\pi \le \pi, \\ \dfrac{2\pi n}{60} t + \varphi_1 + (l-1)\dfrac{2\pi}{z} - 2\pi \\ \quad \text{for } \dfrac{2\pi n}{60} t + \varphi_1 + (l-1)\dfrac{2\pi}{z} \text{ modulo } 2\pi > \pi, \end{cases} \tag{3}$$

where: μ_{l3} – cutting force coefficient for CE no. l as the ratio of forces F_{yl3} and F_{yl1}, k_{dl} – average dynamic specific cutting resistance for CE no. l, b_D – desired undeformed chip width, $h_{Dl}(t)$ – desired undeformed chip thickness for an instantaneous place of CE no. l, f_z – feed per tooth; $f_z = v_f/(zn)$, z – number of the milling tool teeth, κ_r – cutting edge angle, φ_l – instantaneous immersion angle of cutting edge (CE) no. l, n – spindle speed, φ_1 – initial immersion angle of cutting edge (CE) no. 1, φ_{ll} – the lower limit of the immersion angle, φ_{ul} – the upper limit of the immersion angle.

In the orthogonal plane of the tooth (Fig. 2), the clearance (α_0) and rake (γ_0) angles were additionally marked.

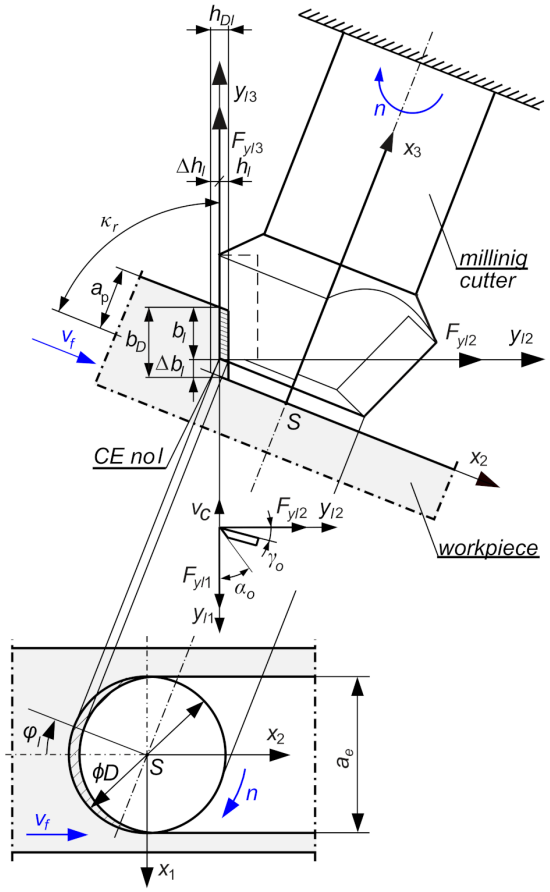

Fig. 2. Face milling scheme [20]

Despite the adopted simplifications, it is worth noting that the proposed description considers the phenomenon of periodic loss of contact between the edge and the workpiece when the instantaneous angle of the edge position is outside the range $\langle\varphi_{ll}, \varphi_{ul}\rangle$.

When milling the surface of large-sized workpieces, the perpendicularity of the main cutting edge of the tool to the machined surface is an important practical case. The above results in the value of the angle $\kappa_r = 90°$. Then the forces $F_{yl3}(t)$ constitute a system of parallel forces that can be reduced to the main (resultant) force and the main moment. Omitting the latter, as of a little importance from the point of view of the interaction between the tool and the workpiece, we obtain the resultant force

perpendicular to the machined surface, with the instantaneous value:

$$F_{y3}(t) = \sum_{l=1}^{i_l} F_{yl3}(t), \tag{4}$$

where: i_l – number of "active" cutting tool edges that have contact with the material at the considered time instant.

In light of the presented considerations, a milled large-size workpiece can be treated as a mass-elastic system with damping, loaded with a resultant periodic cutting force.

Subsequent simplifications, resulting from practical circumstances, concern the adoption of constant values $\mu_{l3}, k_{dl}, b_D, f_z, \kappa_r$ in equations (1) and (2), for all CE no. l. Then, the force acting on the workpiece (4) can be converted to the dimensionless form:

$$f_{y3}(t) = \sum_{l=1}^{i_l} \begin{cases} \cos\varphi_l(t), & \varphi_{ll} \le \varphi_l(t) \le \varphi_{ul}, \\ 0, & \varphi_{ll} > \varphi_l(t) \ \vee \ \varphi_l(t) > \varphi_{ul}, \end{cases} \tag{5}$$

where:

$$f_{y3}(t) = \frac{F_{y3}(t)}{\mu_{l3} k_{dl} b_D f_z \sin\kappa_r}. \tag{6}$$

Let us consider the equation of the dynamics of a large-size workpiece, treating it as a stationary linear system modeled discretely with the number of degrees of freedom m, i.e.:

$$\mathbf{M}\ddot{\mathbf{q}} + \mathbf{L}\dot{\mathbf{q}} + \mathbf{K}\mathbf{q} = \mathbf{f}(t), \tag{7}$$

where the matrices of inertia $\mathbf{M}$, damping $\mathbf{L}$, and stiffness $\mathbf{K}$ are matrices with constant coefficients. The vector of generalized displacements $\mathbf{q}$ is presented as:

$$\mathbf{q}(t) = \mathrm{col}\,(q_i(t)), \quad i = 1, \ldots, m \tag{8}$$

and the vector of dimensionless generalized forces $\mathbf{f}(t)$ as:

$$\mathbf{f}(t) = \mathrm{col}\,(f_i(t)), \quad i = 1, \ldots, m. \tag{9}$$

It is easy to see that a specific generalized coordinate i_s, selected from all degrees of freedom $i = 1, \ldots, m$, can be assigned a resultant dimensionless force (6), i.e.:

$$f_{i_s}(t) \equiv f_{y3}(t). \tag{10}$$

In the case of steady state forced vibrations, the vector components of the generalized forces are harmonic functions:

$$f_i(t) = f_i^0 \sin(\omega t + \varphi_i), \quad i = 1, \ldots, m, \tag{11}$$

where: f_i^0 – amplitude of the force acting along the generalized coordinate no. i, φ_i – phase angle of the force acting along the generalized coordinate no. i, ω – angular frequency of the excitation force,

or periodic functions, which, assuming the Dirichlet conditions are fulfilled, can be represented in the form of a Fourier series:

$$f_i(t) = \sum_{\alpha=0}^{\infty} f_{i\alpha}^0 \sin(\omega_\alpha t + \varphi_{i\alpha}), \quad i = 1, \ldots, m, \tag{12}$$

where: $f_{i\alpha}^0$ – amplitude of the harmonic component no. α of the force acting along the generalized coordinate no. i, $\varphi_{i\alpha}$ – phase angle of the harmonic component no. α of the force acting along the generalized coordinate no. i, ω_α – angular frequency of the harmonic component no. α of the excitation force.

In practice, we consider a finite number M of the harmonic components of the series, obtaining:

$$f_i(t) \cong \sum_{\alpha=0}^{M-1} f_{i\alpha}^0 \sin(\omega t + \varphi_{i\alpha}), \quad i = 1, \ldots, m. \tag{13}$$

The solution to the problem of forced vibrations consists in decomposing the excitation vector into harmonic components (in the case of harmonic excitation, it will be one component) [23]. Both sides of the equation of dynamics (7) are presented in the form of M harmonic components of the Fourier series. We then get:

$$\sum_{\alpha=0}^{M-1} \left(-\mathbf{M}\omega_\alpha^2 + \mathbf{L}\mathrm{j}\omega_\alpha + \mathbf{K}\right)\mathbf{q}(\mathrm{j}\omega_\alpha) = \sum_{\alpha=0}^{M-1} \mathbf{f}(\mathrm{j}\omega_\alpha), \tag{14}$$

where: j – imaginary unit.

By comparing both sides of equation (14), we obtain a system of M linear algebraic equations with complex coefficients:

$$\begin{cases} \left(-\mathbf{M}\omega_0^2 + \mathbf{L}\mathrm{j}\omega_0 + \mathbf{K}\right)\mathbf{q}(\mathrm{j}\omega_0) = \mathbf{f}(\mathrm{j}\omega_0), \\ \left(-\mathbf{M}\omega_1^2 + \mathbf{L}\mathrm{j}\omega_1 + \mathbf{K}\right)\mathbf{q}(\mathrm{j}\omega_1) = \mathbf{f}(\mathrm{j}\omega_1), \\ \vdots \\ \left(-\mathbf{M}\omega_{M-1}^2 + \mathbf{L}\mathrm{j}\omega_{M-1} + \mathbf{K}\right)\mathbf{q}(\mathrm{j}\omega_{M-1}) = \mathbf{f}(\mathrm{j}\omega_{M-1}). \end{cases} \tag{15}$$

The solutions are vectors $\mathbf{q}(\mathrm{j}\omega_0), \mathbf{q}(\mathrm{j}\omega_1), \ldots, \mathbf{q}(\mathrm{j}\omega_{M-1})$, which can be obtained using, for example, the Gaussian elimination method. As a result, we will get:

$$\begin{cases} \mathbf{q}(\mathrm{j}\omega_0) = \mathbf{H}(\mathrm{j}\omega_0)\mathbf{f}(\mathrm{j}\omega_0), \\ \mathbf{q}(\mathrm{j}\omega_1) = \mathbf{H}(\mathrm{j}\omega_1)\mathbf{f}(\mathrm{j}\omega_1), \\ \vdots \\ \mathbf{q}(\mathrm{j}\omega_{M-1}) = \mathbf{H}(\mathrm{j}\omega_{M-1})\mathbf{f}(\mathrm{j}\omega_{M-1}), \end{cases} \tag{16}$$

where:

$$\mathbf{H}(\mathrm{j}\omega_\alpha) = \left(-\mathbf{M}\omega_\alpha^2 + \mathbf{L}\mathrm{j}\omega_\alpha + \mathbf{K}\right)^{-1}, \quad \alpha = 0, \ldots, M-1 \tag{17}$$

is the dynamic compliance matrix. The element of this matrix, located in row no. i and column no. j means the influence of the force acting along the generalized coordinate no. j on the displacement observed along the generalized coordinate no. i. That is:

$$q_i(\mathrm{j}\omega_\alpha) = H_{ij}(\mathrm{j}\omega_\alpha) f_i(\mathrm{j}\omega_\alpha), \quad \alpha = 0, \ldots, M-1 \tag{18}$$

and $\alpha H_{ij}(\mathrm{j}\omega_\alpha)$ is the FRF between the excitation acting along generalized coordinate no. j and the response observed along generalized coordinate no. i.

Determining the spectrum of displacements $\alpha q_i(\mathrm{j}\omega_\alpha)$ of selected points no. i of the workpiece consists of multiplying the FRF of the workpiece $\alpha H_{ij}(\mathrm{j}\omega_\alpha)$ by the force spectrum $\alpha f_j(\mathrm{j}\omega_\alpha)$ of the mutual interaction of the tool and workpiece.

The latter is obtained by transforming the periodic time function $f_{y3}(t)$ (5) into the domain of frequency ω_α. The q_i function resulting from FRF and force spectrum multiplication is named clamping selection function (CSF) for this research. To estimate the vibration level for a selected clamping condition, the RMS value of vibration is calculated directly from CSF, i.e. without transformation of CSF to the time domain. The obtained value is called the clamping selection indicator (CSI). The clamping condition having the lowest value of this indicator should result in the lowest vibration level during milling of the workpiece for which the CSF was obtained and, earlier, CSI was calculated. However, it must be underlined, that CSI value is only an indicator for comparing various clamping conditions and it is not a prediction of the actual, absolute value of vibration level.

3. RESULTS

3.1. Experimental setup

Milling experiments were performed on a large workpiece made of STW22 03M steel (mass 370 kg, external length 2061 mm, width 1116 mm, height 540 mm) (Fig. 3). The workpiece, which was selected from the actual production plan of the cooperating industry, was fixed on the MIKROMAT 20 V milling center table.

During the experiments, face milling was performed for surfaces 1 and 2 (Fig. 3b). The length of both surfaces was 1778.5 mm. The width of surface 1 was 58 mm (Fig. 4a) and of surface 2 – 55 mm (Fig. 4b). One complete milling operation for surface 1 consists of two steps: 1 – full slot face milling, starting from the left side of the workpiece (i.e. near the sensor no. 22), 2 – down milling performed in the opposite direction. The Sandvik R390-044C4-11M060 tool (diameter ϕ 44 mm, four R390-11 T3 08M-PM 1130 cutting inserts with 0.8 mm nose radius, 12° helix angle of the main cutting edge, cutting edge angle $\kappa_r = 90°$) was used for these operations. For surface 2, the down milling was performed starting from the left side of the workpiece (i.e. near the sensor no. 18). The Sandvik R390-125Q40-17H tool (diameter ϕ 125 mm, eleven R390-17 04 08M-PM 1130 cutting inserts with 0.8 mm nose radius, 17° helix angle of the main cutting edge, cutting edge angle $\kappa_r = 90°$) was used.

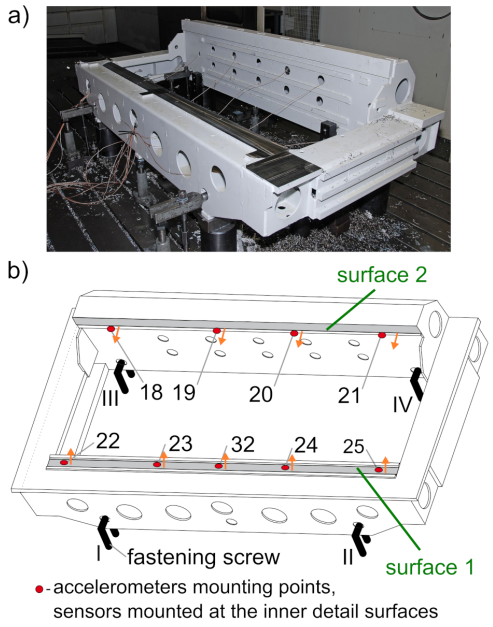

Fig. 3. Research object: workpiece fixed on the table of milling center (a), simplified workpiece scheme with sensors positions and mounting screws marked (b) [20]

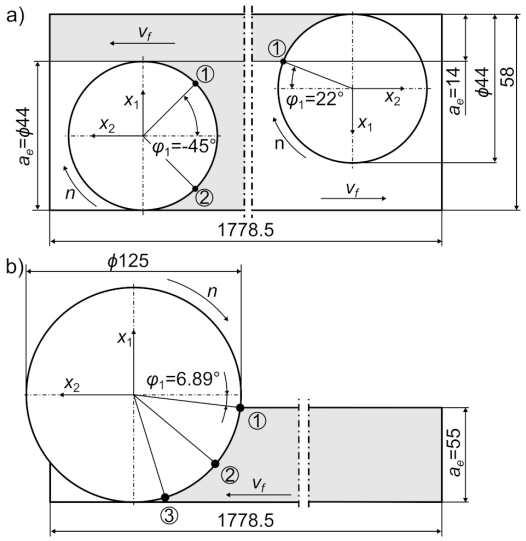

Fig. 4. A scheme of face milling for: surface 1 full slot milling pass on the left, and the down milling pass on the right side (a), surface 2 down milling (b); the positions of the cutting teeth in contact with the material are described by the numbers in circles

Acceleration signals were recorded with a sampling frequency of 10 kHz. The hardware and software configuration of the measurement equipment is described in [24].

Dynamic properties of the workpiece were determined by experimental modal analysis and calculation of frequency response functions (FRFs). The FRF values were calculated with the H3 estimator (averaged values obtained from H1 and H2 estimators) with a resolution of 0.5 Hz.

To record vibration during milling, there were five (for surface 1) and four (for surface 2) accelerometers distributed along the milled surface, on the inner side of the workpiece (Fig. 3b). However, FRFs were determined only for the central part of each surface. Excitations were applied near the sensor numbers 32 and 19 and responses were measured by those sensors, respectively. This was considered sufficient because earlier tests showed that the vibrations in the central part of each surface are the highest (compared to other surface zones) and the level of vibration measured for the central sensor well corresponds with the average level of vibrations observed throughout the milling of the whole surface.

Selected support configurations differed in the tightening torques of the fastening screws (I–IV, Fig. 3b). To apply the desired torque, the dynamometric spanner was used. The configuration of the remaining 11 workpiece supports (not marked in Fig. 3 for clarity) and their tightening torques did not change during the research.

3.2. Cutting force simulation

In order to obtain the cutting force amplitude spectrum, force values with respect to time were calculated (Fig. 5). It must be noted that they are calculated as dimensionless values because calculations are based on the tool and workpiece geometry only and omit various elements such as, for example, specific dynamic cutting pressure and regeneration phenomena.

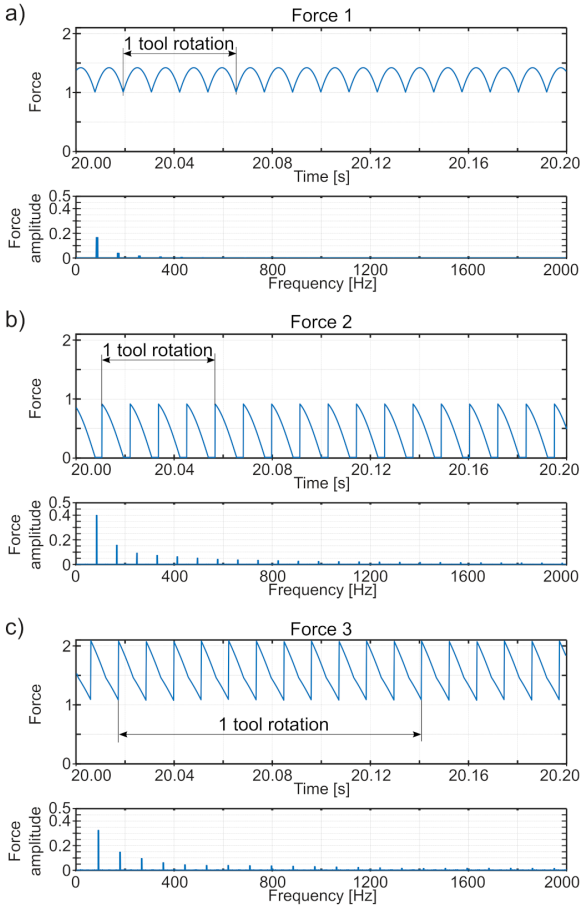

Fig. 5. Fragments of cutting force time plots and spectrum plots for Force 1 – surface 1, full slot milling (a), Force 2 – surface 1, down milling (b), Force 3 – surface 2, down milling (c)

However, such calculated values are proportional (though with some unknown multiplier) to the real ones. This will be further proved, that it is sufficient for comparing various workpiece supports and milling process configurations.

3.3. Cutting force spectrum estimation

As it was said earlier, the key idea of the proposed method is to calculate CSF, i.e. multiply workpiece FRFs obtained for the selected, various configurations (i.e. cases of tightening) of the workpiece by the force spectrum to estimate the spectrum of the resulting vibrations. The result (CSF) does not present accurate amplitude values of vibration frequency components, but they are proportional to them with respect to some unknown multiplier. In the next step, CSI is obtained as the RMS value calculated directly from the spectrum. Comparing CSI values, obtained for each selected workpiece tightening setup, allows for selection of the best setup within the set of considered setups. Figures 6–8 present FRFs, calculated forces spectra and resulting CSFs for selected workpiece tightening setups.

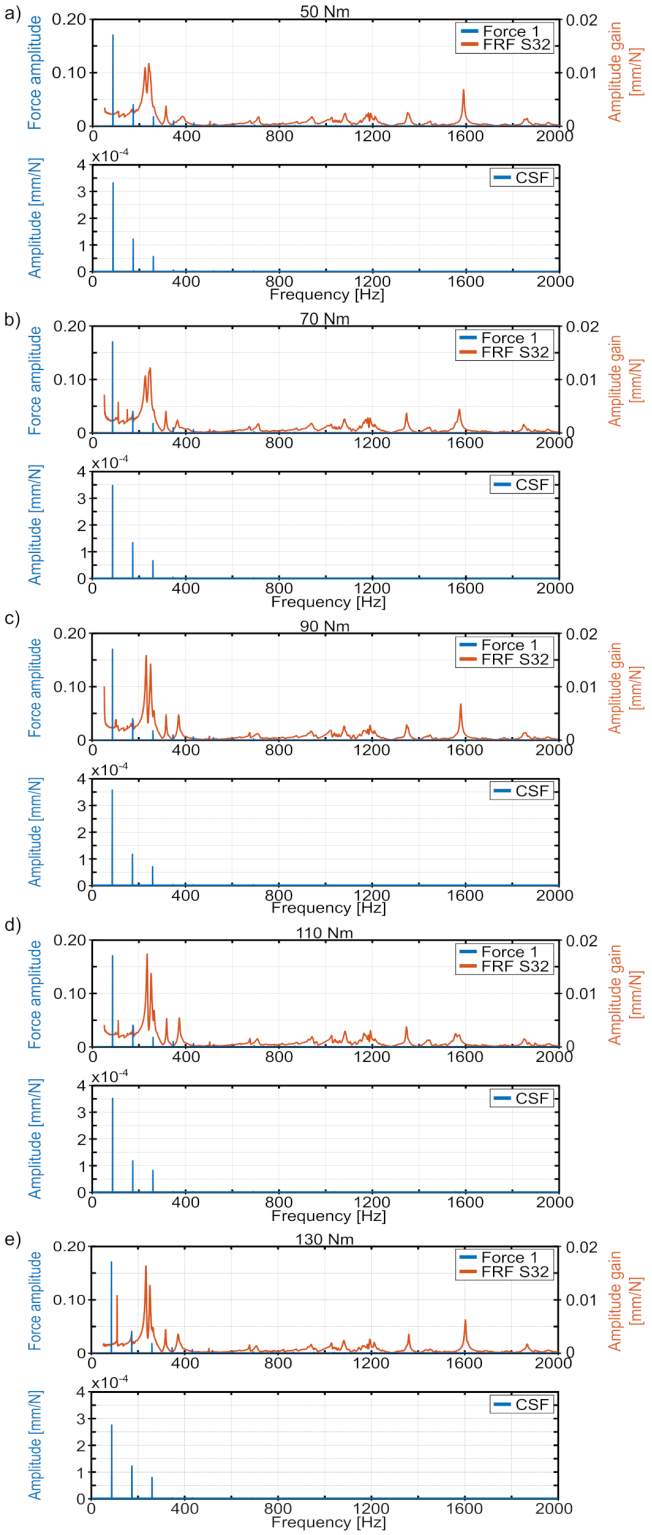

Fig. 6. Surface 1 FRFs with calculated Force 1 spectrum overlaid and the resulting Clamping Selection Functions (CSFs) for selected workpiece tightening setups: 50 Nm (a), 70 Nm (b), 90 Nm (c), 110 Nm (d), 130 Nm (e)

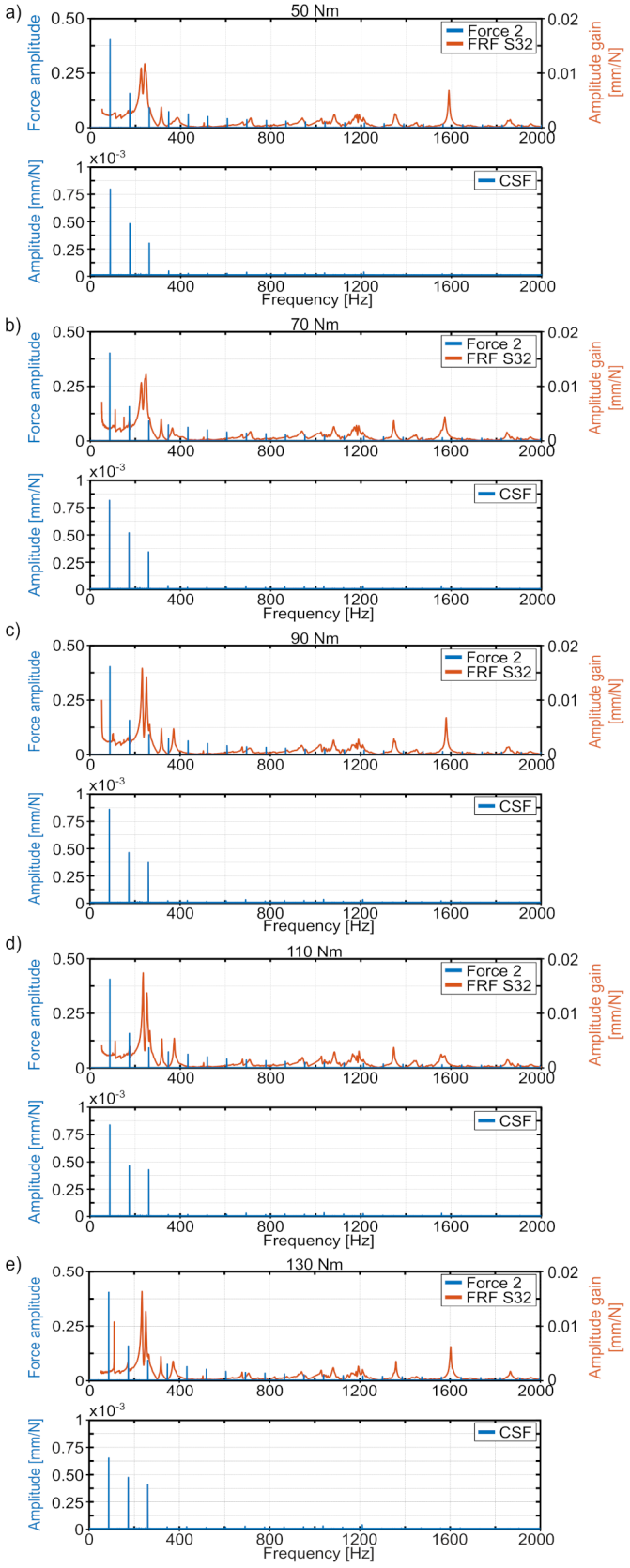

Fig. 7. Surface 1 FRFs with calculated Force 2 spectrum overlaid and the resulting Clamping Selection Functions (CSFs) for selected workpiece tightening setups: 50 Nm (a), 70 Nm (b), 90 Nm (c), 110 Nm (d), 130 Nm (e)

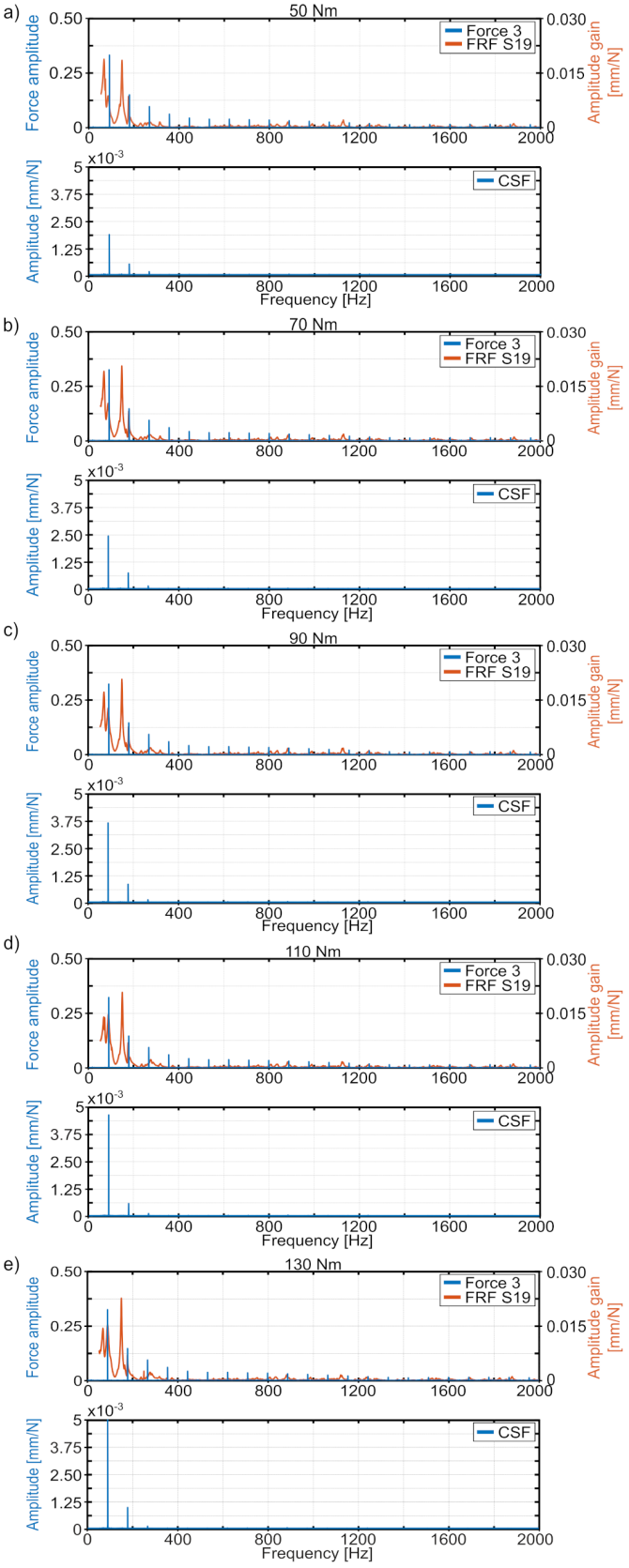

Fig. 8. Surface 2 FRFs with calculated Force 3 spectrum overlaid and the resulting Clamping Selection Functions (CSFs) for selected workpiece tightening setups: 50 Nm (a), 70 Nm (b), 90 Nm (c), 110 Nm (d), 130 Nm (e)

3.4. The verification of estimation results

To verify the results of the described method, an appropriate milling was performed on the real workpiece. Full results are presented in Tables 1 and 2 and some selected plots are presented in Figs. 9–11. The results consist of vibration displacement RMS calculated for the milling process fragment when the tool was in the vicinity of subsequent sensors as well as the average value for the whole milling pass.

Vibration level estimation (CSI) obtained by the proposed method is also presented.

Additionally, vibration levels observed for the middle sensor, the average value, and the estimation are normalized according to the formula:

$$\underline{x} = \frac{x - \bar{x}}{\sigma}, \tag{19}$$

where: $\bar{x}$ –average value and σ – the standard deviation of the set of results obtained for the selected workpiece tightening setup.

This was done for a clearer presentation of trends in the results and to allow a comparison of results. Normalized values are also presented in Fig. 12. Additionally, results in the table confirm

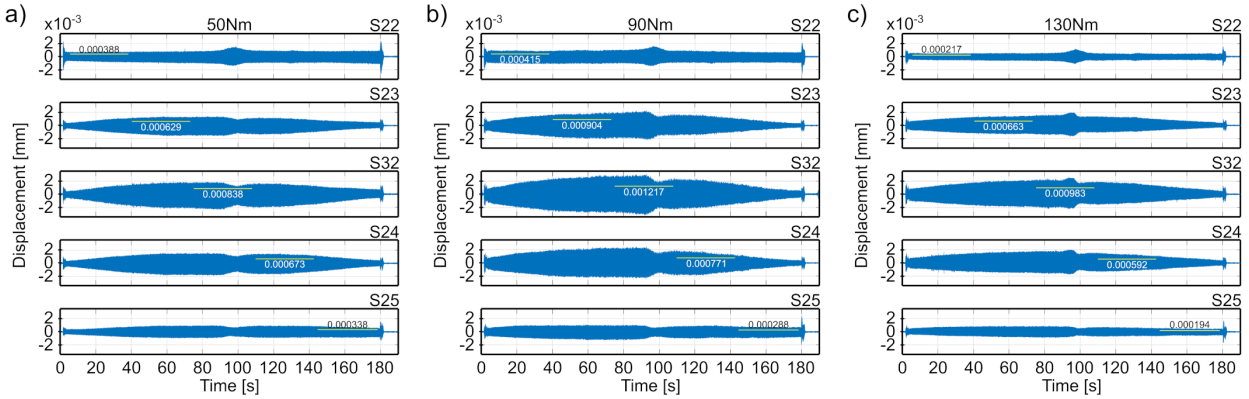

Fig. 9. Workpiece vibrations (displacements) during full milling of surface 1, fixing tightening torque: 50 Nm [20] (a), 90 Nm (b), 130 Nm (c)

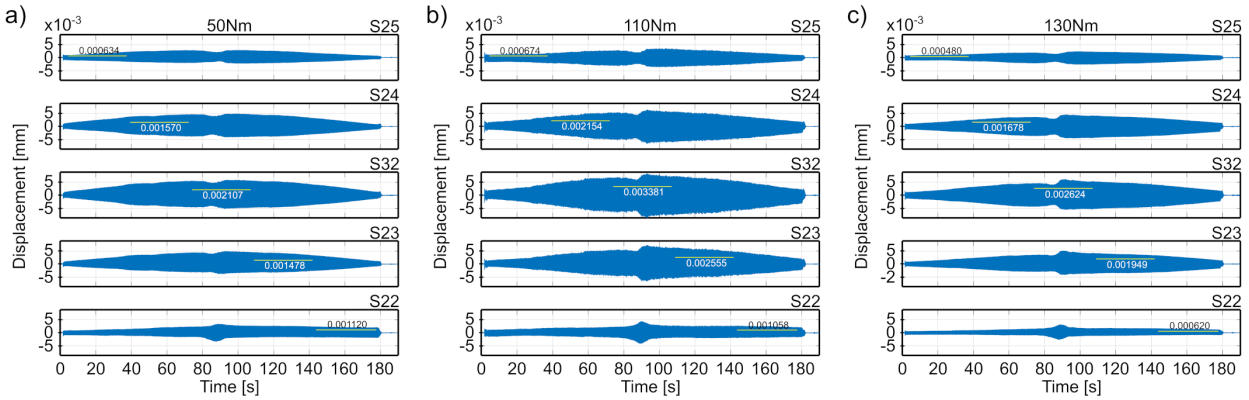

Fig. 10. Workpiece vibrations (displacements) during down milling of surface 1, fixing tightening torque: 50 Nm [20] (a), 110 Nm [20] (b), 130 Nm (c)

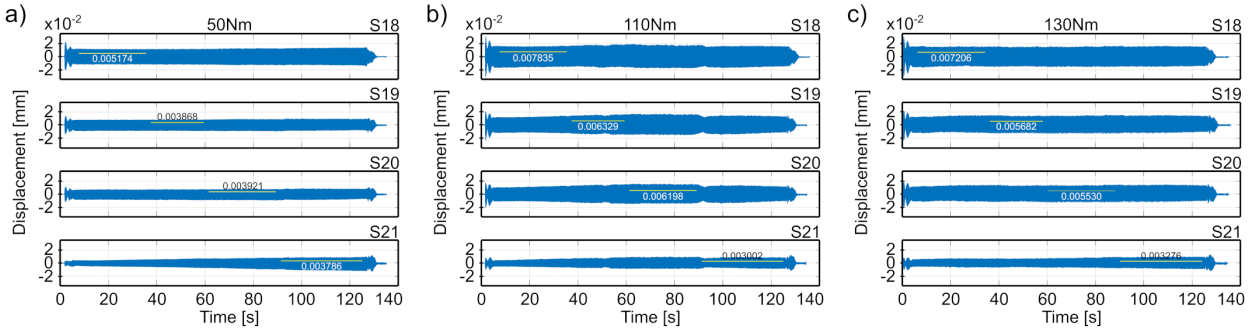

Fig. 11. Workpiece vibrations (displacements) during down milling of surface 2, fixing tightening torque: 50 Nm (a), 100 Nm (b), 130 Nm (c)

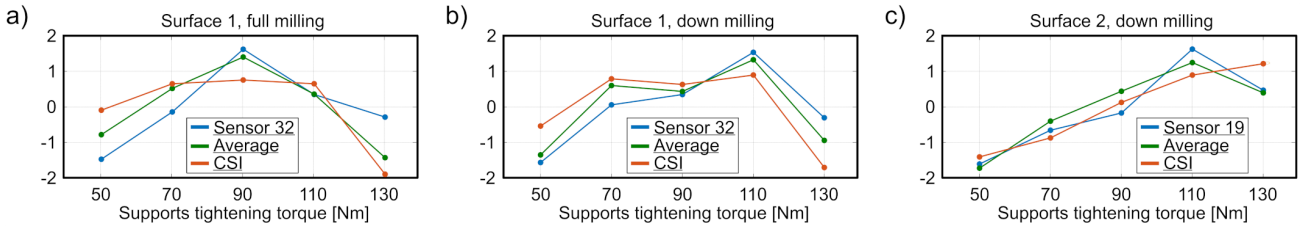

Fig. 12. Normalized results for vibration RMS observed near the middle sensor, average vibration RMS and vibration level estimation (CSI) for Force 1 - surface 1 full milling (a), Force 2 - surface 1, down milling (b), Force 3 - surface 2 down milling (c)

Table 1

RMS values of the displacements (vibrations) during full and down milling of surface 1 for selected fixing conditions [20]. The lowest (best) values marked as bold, the highest values marked as italic. Symbol in Dir. column indicates tool movement direction

Surface 1	Full milling						Down milling					
Torque [Nm]	Dir.	50	70	90	110	130	Dir.	50	70	90	110	130
		RMS [νm]						RMS [νm]				
Sensor 22	⇓	0.388	0.528	0.415	0.405	**0.217**	⇑	*1.120*	1.326	1.036	1.058	**0.620**
Sensor 23		**0.629**	0.737	*0.904*	0.732	0.663		**1.478**	2.009	2.121	*2.555*	1.949
Sensor 32		**0.838**	1.001	*1.217*	1.061	0.983		**2.107**	2.774	2.893	*3.381*	2.624
Sensor 24		0.673	0.702	*0.771*	0.706	**0.592**		**1.570**	2.042	2.068	*2.154*	1.678
Sensor 25		0.338	0.332	0.288	0.342	**0.194**		0.634	0.876	0.734	0.674	**0.480**
Average [μm]		0.573	0.660	*0.719*	0.649	**0.530**		**1.382**	1.807	1.770	*1.964*	1.470
CSI [mm/N]		0.254	0.268	*0.270*	0.268	**0.220**		0.682	0.732	0.726	*0.736*	**0.638**
		Normalized results						Normalized results				
Sensor 32		**−1.483**	−0.155	*1.605*	0.334	−0.301		**−1.575**	0.044	0.333	*1.518*	−0.320
Average		−0.793	0.505	*1.386*	0.343	**−1.441**		**−1.360**	0.582	0.422	*1.312*	−0.955
CSI		−0.106	0.635	*0.741*	0.635	**−1.906**		−0.551	0.774	0.615	*0.880*	**−1.717**

Table 2

RMS values of the displacements (vibrations) during down milling of surface 2 for selected fixing conditions. The lowest (best) values marked as bold, the highest values marked as italic. Symbol in Dir. column indicates tool movement direction

Surface 1	Down milling					
Torque [Nm]	Dir.	50	70	90	110	130
		RMS [νm]				
Sensor 18	⇓	**5.174**	6.694	*8.143*	7.833	7.206
Sensor 19		**3.868**	4.766	5.357	*6.329*	5.682
Sensor 20		**3.921**	4.426	4.804	*6.198*	5.300
Sensor 21		*3.786*	3.712	3.204	**3.002**	3.276
Average [μm]		**4.187**	4.900	5.377	*5.841*	5.366
CSI [mm/N]		**1.343**	1.806	2.671	3.336	*3.613*
		Normalized results				
Sensor 19		**−1.594**	−0.647	−0.162	*1.628*	0.475
Average		**−1.693**	−0.419	0.434	*1.263*	0.415
CSI		**−1.394**	−0.861	0.135	0.900	*1.219*

that average vibration levels for the whole surface are correlated with vibration levels observed for the central sensor.

4. DISCUSSION OF THE RESULTS

Figure 12 reveals that trends illustrating vibration levels (CSI) for experimental results obtained for centrally located sensors (i.e. sensors 32 and 19) are similar to trends for average vibration levels calculated using all sensors. This means, that estimation based only on FRF for a central sensor is sufficient for the assessment of vibration level for a whole machined surface for a workpiece considered in this research. Normalized CSI estimation results are also generally consent with normalized experimental results. This means, that the proposed method may be used for the selection of the clamping conditions for minimizing vibrations during milling.

Despite some simplifications concerning the stationarity of the computational model of the large-size workpiece milling dynamics, the results of using the described method more accurately predict the best and worst variant of workpiece clamping compared to minimizing the work of cutting forces (MWCF) [19, 20]. And so, for full milling of surface 1, the best clamping variant was obtained when the screws were tightened

with a torque of 130 Nm, and the worst – when tightened with a torque of 90 Nm. However, using the MWCF, a variant of tightening with a torque of 50 Nm (match only in the case of the result recorded with the accelerometer 32) and 110 Nm was obtained, respectively.

For down milling of surface 1, the best variant turned out to be tightening with a torque of 130 Nm (close prediction, but not very accurate), and the worst variant – tightening with a torque of 110 Nm. Using the MWCF method, 50 Nm (much better prediction) and 110 Nm (the identical one) were obtained, respectively [19, 20].

For down milling of surface 2, the best variant turned out to be tightening with a torque of 50 Nm, and the worst variant – with a torque of 130 Nm (prediction close to 110 Nm in machining, but still incorrect). However, in the case of the MWCF method, tightening torques of 50 Nm (identical) and 130 Nm (also the same) were obtained, respectively [19, 20].

The different CSI values (Fig. 12), which determine the highest vibration level, are influenced by the different analytically determined cutting force amplitude spectra for surfaces 1 and 2, and the different FRFs measured on the workpiece that reflect different dynamic properties of both surfaces. Hence, the highest vibration level for each surface is observed at different tightening torque values, i.e. 70–110 Nm for surface 1 and 130 Nm for surface 2.

Despite the fulfillment of the conditions for the repeatability of the FRF obtained in the case of individual tightening torques, there is no explicit analytical relationship between the vibration level index (CSI) and the value of this torque. Different CSIs, with the cutting force spectrum unchanged, are influenced by different FRF spectra, the course of which is influenced by the amplitudes not only for the frequencies corresponding to the poles but also for other frequencies. It is not directly the tightening torque that determines vibration level, but the mutual relations between FRFs and force spectrum amplitudes (positions of peaks and valleys in both frequency functions). And the only source of information about the FRF spectrum is a material experiment. Hence, although intuitively a stronger tightening of the fixtures securing the workpiece should result in a better reduction of vibrations on surface 2, the above is not confirmed by presented CSI values as well as in the experiment carried out in reality. The results of the material experiment showed that the opposite is true.

5. CONCLUSIONS

The article is devoted to the challenge of reducing vibration when milling large-sized workpieces by anticipating the best conditions for fixing the workpiece on the milling machine table. This effective solution is achieved offline, just before commencing the regular milling operations. It relies on a mechanistic model of the cutting process, the determination of frequency response functions (FRF) as a result of modal studies of the workpiece, and simulated waveform of periodically varying nominal cutting forces in time. The proposed approach may be useful for searching for the best conditions for fixing the workpiece on the table. It was not a significant obstacle to omit the change in the configuration of the vibrating system, as well as the dynamic changes in the geometry of the undeformed chip.

The results acquired from the analysis of tool-workpiece vibrations in the face milling process, which were assessed using the RMS values of vibrations, confirm better capability for selecting the best workpiece clamping settings than in the case of the method described in [19, 20]. The estimation with the proposed method improves the accuracy of the prediction, especially for full milling (larger immersion angles). However, the more in the direction of down milling, the more justified use of the MWCF may be observed.

The efficiency of vibration reduction was proved during real milling experiments performed on large-size workpieces, for selected clamping conditions. Calculation of CSF and, subsequently, CSI is relatively straightforward. The only time-consuming part of the whole process is the performance of the experimental modal analysis for a set of initially pre-selected clamping conditions.

ACKNOWLEDGEMENTS

The research was possible thanks to the financial support of the Polish National Centre for Research and Development, project TANGO1/266350/NCBR/2015. Experiments on the MIKROMAT 20V machining center were performed in cooperation with the PHS HYDROTOR Inc. in Tuchola, Poland.

AUTHOR CONTRIBUTIONS STATEMENT

Conceptualization, K.K. and K.J.; Methodology, K.K., M.G., N.S.-M. and K.J.; Validation, K.K., M.G., N.S.-M., K.J. and M.M.; Investigation, K.K., M.G., N.S.-M. and M.M.; Data curation, M.G., N.S.-M. and M.M.; Writing – original draft preparation, K.K., M.G., N.S.-M.; Writing – review & editing, K.K., M.G., N.S.-M., K.J. and M.M.; Visualization M.G.; Project administration, K.K.; Funding acquisition, K.K.

REFERENCES

[1] J. Fei, F. Xu, B. Lin, and T. Huang, "State of the art in milling process of the flexible workpiece," *Int. J. Adv. Manuf. Tech.*, vol. 109, pp. 1695–1725, 2020, doi: 10.1007/s00170-020-05616-z.

[2] G. Li, S. Du, B. Wang, J. Lv, and Y. Deng, "High Definition Metrology-Based Quality Improvement of Surface Texture in Face Milling of Workpieces with Discontinuous Surfaces," *J. Manuf. Sci Eng.-Trans. ASME.*, vol. 144, p. 031001, 2022. doi: 10.1115/1.4051883.

[3] D. Li, H. Cao, J. Liu, X. Zhang, and X. Chen, "Milling chatter control based on asymmetric stiffness," *Int. J. Mach. Tools. Manuf.*, vol. 147, p. 103458, 2019, doi: 10.1016/j.ijmachtools.2019.103458.

[4] H. Liu *et al.*, "Pretightening sequence planning of anchor bolts based on structure uniform deformation for large CNC machine tools," *Int. J. Mach. Tools. Manuf.*, vol. 136, pp. 1–18, 2019, doi: 10.1016/j.ijmachtools.2018.09.002.

[5] G. Li, S. Du, D. Huang, C. Zhao, and Y. Deng. "Elastic mechanics-based fixturing scheme optimization of variable stiffness structure workpieces for surface quality improvement," *Precis Eng.*, vol. 56, pp. 343–363, 2019, doi: 10.1016/j.precisioneng.2019.01.004.

[6] Y. Xiao, Z. Jiang, Q. Gu, W. Yan, and R. Wang, "A novel approach to CNC machining center processing parameters optimization considering energy-saving and low-cost," *J. Manuf Syst.*, vol. 59, pp. 535–548, 2021, doi: 10.1016/j.jmsy.2021.03.023.

[7] X. Zhang, T. Yu, Y. Dai, S. Qu, and J. Zhao, "Energy consumption considering tool wear and optimization of cutting parameters in micro milling process," *Int. J. Mech. Sci.*, vol. 178, pp. 105628, 2020, doi: 10.1016/j.ijmecsci.2020.105628.

[8] K.J. Kaliński, M.A. Galewski, M.R. Mazur, and N. Morawska, "A technique of experiment aided virtual prototyping to obtain the best spindle speed during face milling of large-size structures," *Meccanica*, vol. 56, pp. 825–840, 2021, doi: 10.1007/s11012-020-01214-1.

[9] A. Rubio-Mateos, A. Rivero, E. Ukar, and A. Lamikiz, "Influence of elastomer layers in the quality of aluminum parts on finishing operations," *Metals*, vol. 8, p. 289, 2020, doi: 10.3390/met10020289.

[10] I. Del Sol, A. Rivero, L. N. López de Lacalle, and A.J. Gamez, "Thin-Wall Machining of Light Alloys: A Review of Models and Industrial Approaches," *Materials*, vol. 12, p. 2201, 2019, doi: 10.3390/ma1212201.

[11] M. Meshreki, H. Attia, and J. Kövecses, "Development of a new model for the varying dynamics of flexible pocket-structures during machining," *J. Manuf. Sci. Eng.*, vol. 133, p. 041002, 2011, doi: 10.1115/1.4004322.

[12] A. Mahmud, J.R.R. Mayer, and L. Baron, "Magnetic attraction forces between permanent magnet group arrays in a mobile magnetic clamp for pocket machining," *CIRP J. Manuf. Sci. Technol.*, vol. 11, pp. 82–88, 2105, doi: 10.1016/j.cirpj.2015.08.005.

[13] M. Wan, X.-B. Dang, W.-H. Zhang, and Y. Yang, "Chatter suppression in the milling process of the weakly-rigid workpiece through a moving fixture," *J. Mat. Proc. Techn.*, vol. 299, 2022, 117293, doi: 10.1016/j.jmatprotec.2021.117293.

[14] G. Weicheng, Z. Yong, J. Xiaohui, Y. Ning, W. Kun, and L. Xiao, "Improvement of stiffness during milling thin-walled workpiece based on mechanical/magnetorheological composite clamping," *J. Manuf. Process.*, vol. 68, pp. 1047–1059, 2021, doi: 10.1016/j.jmapro.2021.06.039.

[15] Y. Cai, Z. Zhang, X. Xi, and D. Zhao, "A Deformation Control Method in Thin-Walled Parts Machining Based on Force and Stiffness Matching Via Cutter Orientation Optimization," *J. Manuf. Sci. Eng.*, vol. 145, 2023.

[16] Z.Y. Liu *et al.*, "Energy consumption characteristics in finish hard milling," *J. Manuf. Process.*, vol. 35, pp. 500–507, 2018, doi: 10.1016/j.jmapro.2018.08.036.

[17] M. Casuso, A. Rubio-Mateos, F. Veiga, and A. Lamikiz, "Influence of Axial Depth of Cut and Tool Position on Surface Quality and Chatter Appearance in Locally Supported Thin Floor Milling," *Materials*, vol. 15, p. 731, 2022, doi: 10.3390/ma15030731.

[18] D.Y. Pimenov, M. Kumar Gupta, L.R.R. da Silva, M. Kiran, N. Khanna, and G.M. Krolczyk, "Application of measurement systems in tool condition monitoring of Milling: A review of measurement science approach," *Measurement*, vol. 199, p. 1503, 2022, doi: 10.1016/j.measurement.2022.111503.

[19] N. Stawicka-Morawska, "The method of selecting the stiffness of fastening a large-size workpiece in application to vibration reduction during milling with multi-edge tools", PhD Thesis, Gdańsk University of Technology, 2022. (in Polish)

[20] K.J. Kaliński, N. Stawicka-Morawska, M.A. Galewski, and M.R. Mazur. "A method of predicting the best conditions for large-size workpiece clamping to reduce vibration in the face milling process," *Sci Rep.*, vol. 11, p. 20773, 2021, doi: 10.1038/s41598-021-00128-6.

[21] S. Zeng, X. Wan, W. Li, Z. Yin, and Y. Xiong, "A novel approach to fixture design on suppressing machining vibration of flexible workpiece," *Int. J. Mach. Tools. Manuf.*, vol. 58, pp. 29–43, 2012, doi: 10.1016/j.ijmachtools.2012.02.008.

[22] G. Li, S. Du, D. Huang, C. Zhao, and Y. Deng, "Elastic mechanics-based fixturing scheme optimization of variable stiffness structure workpieces for surface quality improvement," *Prec. Eng.*, vol. 56, pp. 343–363, 2019, doi: 10.1016/j.precisioneng.2019.01.004.

[23] K. Kaliński, "The finite element method application to linear closed loop steady system vibration analysis," *Int. J. Mech. Sci.*, vol. 39, pp. 315–330, 1997, doi: 10.1016/S0020-7403(96)00032-X.

[24] M.A. Galewski, "Application of the LabVIEW environment for experimental modal analysis support," in *From Finite Element Method to Mechatronics*. K.J. Kalinski, K. Lipinski, Eds., Gdansk: The Publication of Gdansk University of Technology, 2017, pp. 105–118. (in Polish)